Journal of Current Medical Research and Opinion
Received 15-04-2022| Revised 20-04-2022| Accepted 08-05-2022| Published Online 10-08-2023

DOI: https://doi.org/10.52845/CMRO/2023/6-8-4 ISSN (O) 2589-8779 | (P) 2589-8760

CMRO 06 (08), 1649-1670 (2023)

Original Research

Identification and Characterisation of a cyclic di-GMP-specific Diguanylate Cyclase and Phosphodiesterase Genes in *Klebsiella Pneumoniae* MBB9

Ghazay F. Alotaibi[1] * | Jeff Green[2]

[1]Department of Environment and Marine Biology, Saline Water Desalination Technologies Research Institute, P.O. 8328 Al-Jubail 31951, Saudi Arabia,
[2]Department of Molecular Biology and Biotechnology, The University of Sheffield, Sheffield S10 2TN, United Kingdom

Abstract:

Bis-(3'–5')-cyclic-dimeric guanosine monophosphate (c-di-GMP) is a bacterial second messenger known to mediate the regulation of multiple cellular processes, including bacterial adhesion and biofilm formation, bacterial motility, and control the virulence of bacterial pathogens. In many bacteria, the second messenger c-di-GMP, an intracellular signalling molecule, plays a key role in the lifestyle changes and controls the transition between the motile planktonic and sessile biofilm lifestyles. The intracellular levels of c-di-GMP are controlled by c-di-GMP synthesis and degradation catalyzed by diguanylate cyclase (DGC) and phophodiesterase (PDE) enzymes. The GGDEF protein domain synthesizes cyclic di-GMP, whereas the EAL and HD-GYP domains are involved in cyclic di-GMP hydrolysis. Various bacteria contain many copies of these proteins with a diverse organizational structure that highlights the complex regulatory mechanisms of this signaling network. The whole genome of *Klebsiella pneumoniae* MBB9, recovered from river-stones collected from the Porter Brook, Sheffield, was sequenced and compared to *K. pneumoniae* 342 to identify DGCs and PDEs and analyze the domain structure of such proteins. *Klebsiella pneumoniae* MBB9 harboured multiple copies of proteins with GGDEF and EAL domains, most of these were linked to sensory domains and were found to possess 11 genes with GGDEF domains, 11 genes with EAL domains, and 6 genes with both GGDEF and EAL domains. Thirty-nine percent of these proteins contained the GGDEF sequence motif, whereas 39% had EAL sequence motif, and 21 % were hybrid proteins containing both GGDEF and EAL domains. The majority of GGDEF domains are catalytically active as they have an intact conserved A site, whereas all EAL domains have c-di-GMP PDE activity except BluF_2 and YahA proteins.

Keywords: Biofilm formation*; Klebsiella pneumoniae;* microtiter plate; the second messenger cyclic-di-GMP; whole genome.

1. Introduction:

The pattern of genes expressed in sessile, biofilm-producing bacteria can be different from that of planktonic cells (Marvin *et al*., 2001). Bis-(3'–5')-cyclic-dimeric guanosine monophosphate (c-di-GMP) is a bacterial second messenger known to mediate the regulation of multiple cellular processes (Sisti *et al*., 2013). This molecule was first discovered as an allosteric activator of cellulose synthesis in *Gluconacetobacter xylinus* (Cotter and Stibitz, 2007). Cyclic-di-GMP has been found to regulate a wide range of functions including bacterial adhesion and biofilm formation, bacterial motility, and control the virulence of bacterial pathogens (Sisti *et al*., 2013). The intracellular levels of c-di-GMP are modulated by the opposing action of two enzymatic functions (Schmid *et al*., 2017). Diguanylate cyclases (DGCs) catalyze the synthesis of c-di-GMP from two molecules of GTP and contain a consensus GG(D/E)EF motif catalytic active site (A-site) along with a second RxxD motif product inhibition site (I-site) that allows c-di-GMP binding to regulate the active domain (Cruz *et al*., 2012). Cyclic-di-GMP-specific phosphodiesterases (PDEs) hydrolyze c-di-GMP into linear 5′-phosphoguanylyl-(3′-5′)-guanosine (pGpG) or to two molecules of GMP (Stelitano *et al*., 2013). Cyclic-di-GMP is recognized as an intracellular signalling molecule that modulates the transition between planktonic and sessile bacterial lifestyles (Valentini and Filloux, 2016). High levels of c-di-GMP have been found to enhance the adhesion to surfaces, production of exopolysaccharides (EPS), and formation of bacterial biofilms, whereas low levels can increase bacterial motility, promote biofilm disassembly and lead to the activation of virulence pathways (Cruz *et al*., 2012; Gao *et al*., 2013). Diguanylate cyclases proteins are characterized by a GGDEF catalytic motif which plays a significant role in the activity of these proteins, while PDE activity is associated with C-terminal EAL or HD-GYP domains (Cruz *et al*., 2012). Several studies have shown that besides the C-terminal catalytically active site present in DGC and PDE proteins, most of them harbor N-terminal sensory input domains that can respond to various internal and external signals, triggering activation of DGCs or PDEs (Cruz *et al*., 2012). These domains may be found individually or together as hybrid proteins that possess both GGDEF and EAL domains; however, hybrid proteins usually have only PDE or DGC activity, although in some cases both functions can be present (Cruz *et al*., 2012). Many GGDEF and EAL domain proteins possess sensory domains, indicating that complex signal integration and domain interaction might exist in a single protein (Tchigvintsev *et al*., 2010). Microbial attachment to a host cell and abiotic surfaces is typically mediated in gram-negative enterobacteria by fimbrial adhesins (Murphy *et al*., 2013). Two fimbrial adhesions, type 1 and type 3 fimbriae are usually identified on the surfaces of *K. pneumoniae* (Murphy *et al*., 2013). They are considered virulence factors and play a key role in *K. pneumoniae* biofilm formation (Schroll *et al*., 2010; Alcántar-Curiel *et al*., 2013). The type 3 fimbriae are characterized by their ability to agglutinate erythrocytes treated with tannic acid *in vitro and are* designated as mannose-resistant hemagglutinins (MRHA) are necessary for biofilm formation on abiotic surfaces (Schurtz Sebghati *et al*., 1998; Murphy *et al*., 2013; Vuotto *et al*., 2014). The type 3 fimbriae are synthesized by the chaperone-usher pathway of protein translocation and the gene cluster contains five genes, which encode for structural components of the fimbrial appendage (Figure 5.1) (Jonathan *et al*., 2011). These genes include determinants encoding the major fimbrial subunit (MrkA), a chaperone-usher system (MrkBC, respectively), the fimbrial tip adhesin (MrkD), and a minor fimbrial subunit (MrkF) (Johnson *et al*., 2011). The *mrk* cluster is adjacent to a three-gene cluster that encodes gene products that exhibit amino acid relatedness to other bacterial proteins involved in c-di-GMP sensing and modulation; one of these genes, designated *mrkJ*, exhibits homology to EAL domain-containing PDEs (Johnson and Clegg, 2010). To determine the role of c-di-GMP in *K. pneumoniae* MBB9 biofilm, genomic DNA was extracted and sequenced, genes coding for GGDEF and EAL proteins were identified and quantitative real-time PCR was used to compare the expression of genes coding for GGDEF and EAL proteins in planktonic and sessile cells of *K. pneumoniae* MBB9 adhered to glass wool fibres and glass slide

coupons. Expression of *yhjH_1*, *yhjH_2* and *yhjH_3* was performed and bis(*p*-nitrophenyl) phosphate (BNPP) was used to test the activity of recombinant *K. pneumoniae* MBB9 YhjH proteins.

2. Material and Methods

2.1 Source and Sampling

The same day (March 2015), river-stones (thick, light brown, sticky growth) on the upper surfaces were collected in a sterile plastic container from Porter Brook in Sheffield, United Kingdom, and were stored until analyis in the cool icebox.

2.2 Isolation of bacteria from environmental biofilms

Epilithic biofilms on the stones were scraped and suspensions were serially diluted 1:100 in physiological saline (0.85%) using an aseptic technique (APHA, 1998). Different selective media: R2A agar, Eosin-methylene blue (EMB) agar, MacConkey agar, Xylose lysine deoxycholate (XLD) agar, nutrient agar, and Violet Red Bile Agar were used to inoculate the suspension. The inoculated plates were incubated aerobically at 37ºC for 24–72 h. To obtain pure cultures of the bacterial isolates, colonies with various colors and morphologies were streaked again on freshly agar plates.

2.3 Bacterial morphological and biochemical characterization

Isolated colonies from the agar plates were selected and characterized for preliminary identification using various morphological and biochemical properties (Bergey and Holt, 1994). Morphological parameters, such as colony form, elevation, margin, surface, optical features, consistency and color are used along with biochemical tests, including catalase and oxidase activities.

2.4 Molecular identification of bacteria via 16S rRNA gene sequencing and phylogenetic analysis

GenElute™ Bacterial Genomic DNA Kit was used according to the manufacturer's instructions to extract Bacterial genomic DNA from all isolated bacteria. DNA preparations purity was assessed spectrophotometrically using a Nanodrop 1000 (A260/280) (NanoDrop Technologies, Wilmington, DE, USA). PCR was used to amplify 16S rRNA genes of the bacterial isolates using forward (27F) 5'-AGAGTTTGATCCTGGCTCAG-3' and reverse (1492R) 5'-GGTTACCTTGTTACGACTT-3' primers (universal, 16S rDNA gene) to amplify the V1-V9 region (1500 bp) of the16S rRNA gene. In brief, a master mix of 25 µl total volume was prepared as follows: 12 µl of 2X master mix (BioLabs, England), 2 µl of each oligonucleotide primer (10 µM), 7 µl of Molecular Grade Water and 2 µl of template DNA. All reactions were run on a LabCycler (SensQuest, Germany) under the following conditions: initial denaturation at 98°C for 30 s, 35 cycles of 95°C for 1 min, 58°C for 30 s, 72°C for 5 min and a final extension at 72°C for 5 min followed by a hold at 4°C. The amplified DNA fragments were separated on a 1% (w/v) agarose gel electrophoresis (BIO-RAD, USA). SYBR Safe® (Invitrogen) was used to stain the gels. A UVI tech photodocumentation system was used to visualize DNA bands for viewing the DNA fragments. Following the sequencing, each DNA sequence chromatogram was examined using the bioinformatic tool FinchTV software to evaluate its quality; however, sequences with low quality were trimmed from both ends and moved the remaining good-quality sequences into a new file. Basic local alignment search tool (BLAST) in National Center for Biotechnology Information (NCBI) and Ribosomal Database Project (RDP) were used to produce taxonomic information about the source species. The neighbor-joining method implemented in the program MEGA software was used for construction of phylogenetic tree.

2.5 Assessment of biofilm formation by the isolated bacteria using microtiter plate assay

The microtiter plate method of O'Toole and Kolter (1998) was applied with a few adjustments. Briefly, bacterial isolates were grown overnight in nutrient broth at 37°C. The OD_{600} of the bacterial suspensions

was adjusted to 0.5 McFarland standards (approximately 10^8 CFU/ml). A flat-bottomed polystyrene 96-well microtiter plate (Costar; Corning Incorporated., USA) was used to inoculate aliquots (200 µl). As plate sterility controls, the sterile nutrient broth was used and plates were covered and incubated at 37°C for 24 h (Gomes, 2012). Planktonic cells in the fluid were then removed by inverting the plate and decanting the contents, followed by thoroughly rinsing three times with 200 µl of sterile deionised water (dH_2O) to remove any remaining unattached planktonic cells. The microtiter plates were dried by air at 37°C, and adherent bacteria were stained with 200 µl of 1% (w/v) crystal violet solution (crystal violet; Merck, Germany) for 25 min (Christensen *et al.*, 1985; Christensen, Baldassarri and Simpson, 1995). The supernatant was discarded after the staining step and the wells were rinsed with repeated washing with sterile deionized water (dH_2O) for any excess stain removal. Any biofilm-integrated CV was solubilized by adding 250 µl of 30% glacial acetic acid. A multi-well plate reader (BioTek FLx800, UK) at the absorbance of light at 595 nm was used to assess the CV liberated from the attached material and control wells (Saloni *et al*., 2012).

2.6 Genome sequence of Klebsiella *pneumonia* MBB9

Genomic DNA of *K. pneumoniae* MBB9 was extracted using GenEluteTM Bacterial Genomic DNA kit according to the manufacturer's instructions. The purity of the DNA preparations was assessed spectrophotometrically using a Nanodrop 1000 ($A_{260}/_{280}$) (NanoDrop Technologies, Wilmington, DE, USA) and the ratio of absorbance $A_{260/280}$ was 1.42 ± 0.15. Whole-genome shotgun sequencing was performed on the Illumina HiSeq 2000 sequencer by MicrobesNG (IMI-School of Biosciences, Birmingham, UK).

2.7 Comparative analyses of the complete genome of *K. pneumoniae* MBB9 with *K. pneumoniae* 342 for detection of diguanylate cyclase and phosphodiesterase encoding genes

Comparison of *K. pneumoniae* MBB9 and *K. pneumoniae* 342 strains was performed using the Artemis Comparison Tool (ACT) (www.sanger.ac.uk/software/artemis/ACT) to identify genes coding for GGDEF and EAL proteins that might be conserved in the core genome of *K. pneumoniae* MBB9 isolate compared to the *K. pneumoniae* 342 reference genome. Illumina reads were first assembled into contigs using the program SPAdes through the Galaxy interface (http://usegalaxy.org). The quality of the Fasta file containing the contigs assembled by SPAdes was then assessed using Quast program (http://quast.bioinf.spbau.ru). The quality of SPAdes assembly was further assessed using the program Actcompare via a Galaxy interface (http://usegalaxy.org) which performs a comparison between two genomes using another program, MUMmer and generates a PNG image showing the comparison and an ACT comparison file which can be used in Artemis software (https://www.sanger.ac.uk/science/tools/artemis-comparison-tool-act) that allows users to view an alignment between *K. pneumoniae* MBB9 and *K. pneumoniae* 342 genomes and examine the conserved and variable regions of the genome (Table 1 and Figure 1). Prokka program via the Galaxy interface (http://usegalaxy.org) was then used for automated annotation and the Genbank file generated was used in Artemis to explore the annotated genome.

3. Results:

As described in my previous research, 22 different bacterial strains were isolated and identified from biofilms formed on stones recovered from the Porter Brook, Sheffield. Of the 22 isolates, ten gram-negative potential pathogens were selected and screened for biofilm production (Alotaibi, 2020). The modified microtiter-plate test, as a quantitative assay, showed that all tested strains produced biofilms as the mass of the retained crystal violet stain on the test plate indicated the biofilms presence. *Klebsiella pneumoniae* MBB9 was among these isolates that showed the highest biofilm production in the CV microtiter plate assay (Alotaibi, 2020).

3.1 Genome sequence of *Klebsiella pneumoniae* MBB9

A total of 760,680 reads (~55.5204 -fold coverage) and 132 of contigs (166 to 451,262 bp) were generated. The genome size was 5,822,464 bp containing 56.97% GC.

3.2 Comparative analyses of the complete genome of *K. pneumoniae* MBB9 with *K. pneumoniae* 342 for detection of diguanylate cyclase and phosphodiesterase encoding genes

As shown in Table 1 and Figure 1, the whole-genome comparative analysis of *K. pneumoniae* MBB9 and *K. pneumoniae* 342 was performed using Artemis Comparison Tool (ACT). However, six genes coding for GGDEF and EAL proteins were absent in *K. pneumoniae* MBB9 compared to the genome of the reference strain (Table S1 in supplementary material and Figure 2). The absence of these genes was confirmed by PCR using *K. pneumoniae* 342 gene-specific primers (Table S1 in supplementary material and Figure S2). Thus, *K. pneumoniae* MBB9 possesses 11 genes with GGDEF domains, 11 genes with EAL domains, and 6 genes with both GGDEF and EAL domains (Table 2). Thirty-nine percent of these proteins contained the GGDEF sequence motif, whereas 39% had EAL sequence motif, and 21 % were hybrid proteins containing both GGDEF and EAL domains (Table 2). Table 3 showed the comparison of GGDEF/EAL in *K. pneumoniae* MBB9, *K. pneumoniae* 342 and *K. pneumoniae* MGH 78578.

Table 1: Whole-genome comparative analysis of *K. pneumoniae* MBB9 and *K. pneumoniae* 342 using Artemis Comparison Tool (ACT).

Categories	***K. pneumoniae* 342**	***K. pneumoniae* MBB9**
Number of bases	5641239	5833005
Genes	5425	5586
Gene sequence composition	A (20.7%) C (28.51%) G (29.91%) T (20.86%)	A (20.89%) C (28.32%) G (29.88%) T (20.9%)
GC percentage	58.43%	58.21%

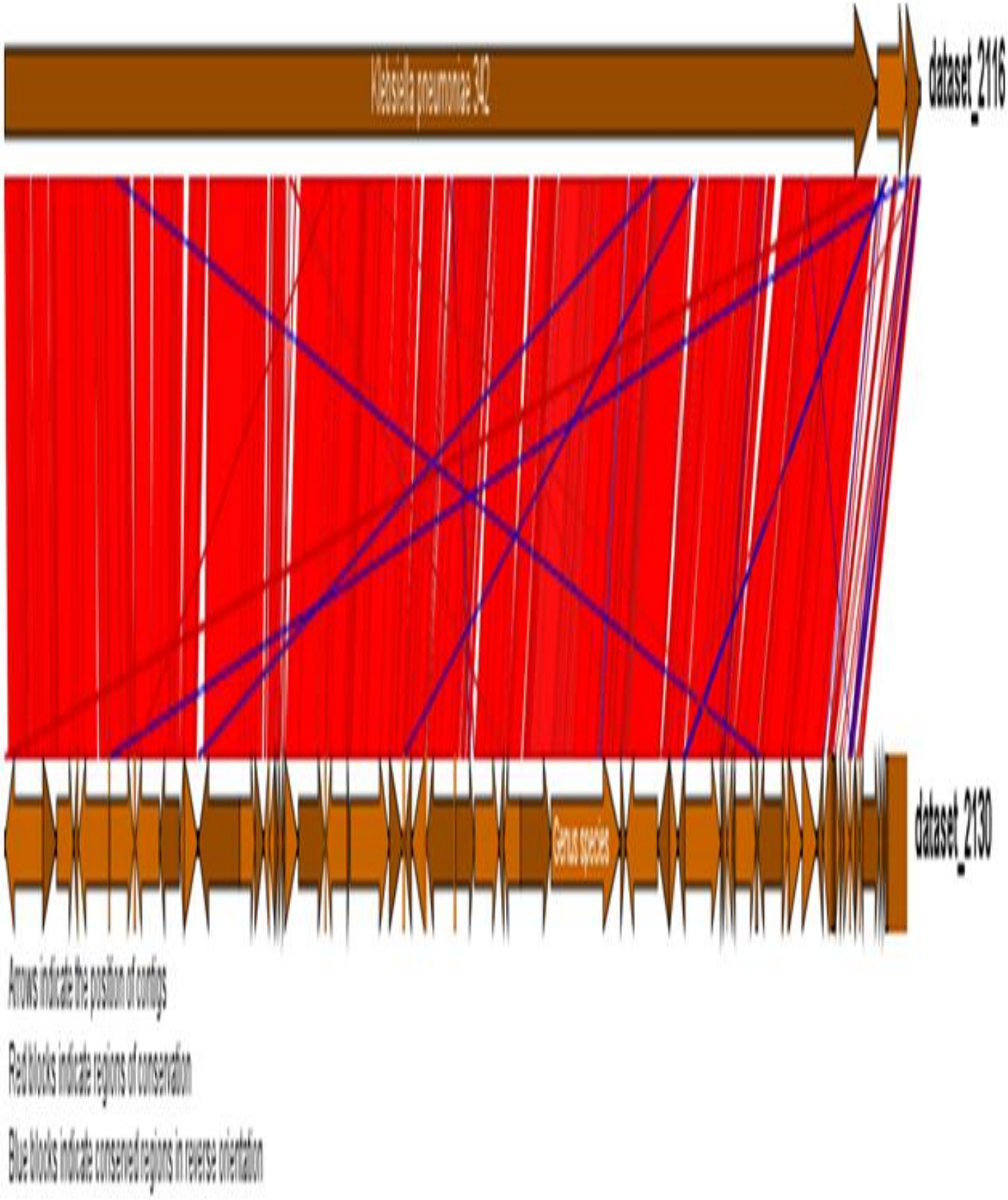

Figure 1: PNG image showing a sequence alignment of *K. pneumoniae* MBB9 and *K. pneumoniae* 342. Upper: *K. pneumoniae* 342 reference strain and lower: *K. pneumoniae* MBB9 linked via the comparison file; red blocks indicate conserved regions in the same orientation, blue indicates conserved regions in the opposite orientation and white indicates no match.

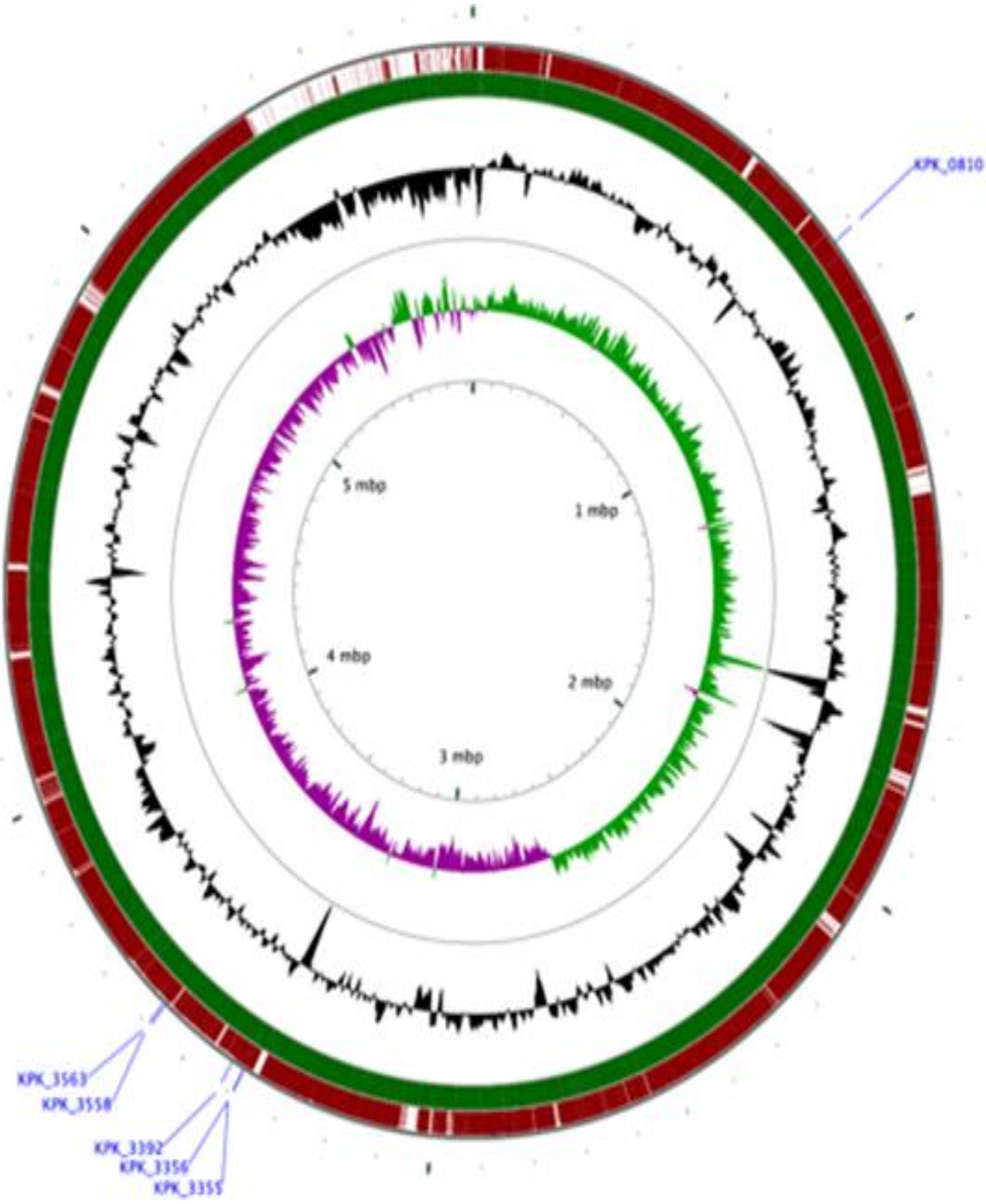

Figure 2: A graphical circular map of *K. pneumoniae* MBB9 genome. Genome synteny between genomes of *K. pneumoniae* MBB9 and *K. pneumoniae* 342. From the outside to the inside: the two outermost circles show the BLASTN homologies between *K. pneumoniae* 342 (red) and *K. pneumoniae* MBB9 (green), the GC contents in black and the GC skew; Green (GC content of the forward strand), Purple (GC content of the reverse strand). The innermost circle the numeric genome position. Comparisons were made using the CGView server (http://wishart.biology.ualberta.ca/cgview/) using partial opacity to visualize overlapping hit.

Table 2: Catalogue of genes coding for GGDEF and EAL proteins in *K. pneumoniae* MBB9.

Number	Gene	Type of protein
1	*KPI_01740* ***yedQ***	GGDEF
2	*KPI_04512* ***dosC***	GGDEF
3	*KPI_02434* ***ydaM***	GGDEF
4	*KPI_02248* ***ycdT_1***	GGDEF
5	*KPI_02576* ***ycdT_2***	GGDEF
6	*KPI_03124* ***vdcA_1***	GGDEF
7	*KPI_04431* ***vdcA_2***	GGDEF
8	*KPI_03117* ***yeaP_2***	GGDEF
9	*KPI_01668* ***yeaP_1***	GGDEF
10	*KPI_01113* ***yfiN***	GGDEF
11	*KPI_04913* ***vdcA_3***	GGDEF
12	*KPI_01662*	GGDEF-EAL-hybrid
13	*KPI_02530*	GGDEF EAL-hybrid
14	*KPI_02680*	GGDEF EAL-hybrid
15	*KPI_01338* ***yfgF_2***	GGDEF-EAL-hybrid
16	*KPI_00464* ***csrD***	GGDEF-EAL-hybrid
17	*KPI_04823* ***yjcC***	EAL
18	*KPI_01488* ***adrB_1***	EAL
19	*KPI_01840* ***adrB_2***	EAL
20	*KPI_03307* ***yahA***	EAL
21	*KPI_03970* ***ylaB***	EAL
22	*KPI_02624* ***bluF_1***	EAL
23	*KPI_03531* ***bluF_2***	EAL
24	*KPI_01254* ***yfgF_1***	GGDEF-EAL-hybrid
25	*KPI_00816* ***yhjH_1***	EAL
26	*KPI_03123*	EAL
27	*KPI_03128* ***yhjH_2***	EAL
28	*KPI_00230* ***bcsB_1***	EAL

Table 3: Comparison of GGDEF/EAL catalogues in *K. pneumoniae* strains.

***K. pneumoniae* MBB9**	***K. pneumoniae* 342**	***K. pneumoniae* MGH 78578**
YhjH_3/PdeH		KPN_03274
CsrD	KPK_0458	KPN_03660
YjcC/PdeC	KPK_5257	KPN_04461
DosC/DgcO	KPK_4891	
YfgF_1/PdeF	KPK_1302	KPN_02828
YfgF_2/PdeA	KPK_1394	KPN_02745
KP_01662	KPK_1732	KPN_02445
YeaP/DgcP	KPK_1739	KPN_02450
YedQ/DgcQ	KPK_1855	KPN_02424
BluF_2	KPK_3794	KPN_00782
YdaM/DgcM	KPK_2566	KPN_01794
YhjH_2	KPK_3327	KPN_01159
BluF_1	KPK_2809	KPN_01598
KP_02680	KPK_2890	
YcdT_2/DgcX-like_2	KPK_2741	KPN_01638
KP_02530	KPK_2691	KPN_01677
YeaP_2/DgcP	KPK_3313	KPN_01172
VdcA_1	KPK_3323	KPN_01163
YahA/PdeL C-TERM ONLY	KPK_3533	KPN-01010
YcdT_1/DgcX-like_1	KPK_2368	KPN_01980
AdrB_2/PdeD	KPK_1962	KPN_02331
YlaB/PdeB	KPK_4255	KPN_00425
AdrB_1/PdeN	KPK_1552	KPN_02609
VdcA_2	KPK_4792	KPN_04822 C-TERM ONLY
YhjH_1/PdeH_1	KPK_0837	KPN_03274
VdcA_3	KPK_5304	KPN_04370
YfiN/DgcN	KPK_1195	KPN_02925
Cph2_1	KPK_0227	KPN_03879
Cph2_2	KPK_3663	KPN_00899
	KPK_3356	
	KPK_3558	

3.3 Identification of domains in GGDEF and EAL containing proteins of *K. pneumoniae* MBB9

To further characterize the GGDEF and EAL domain proteins of *K. pneumoniae* MBB9, signal peptides, conserved and sensor domains were identified. As shown in Table 4, most of the *K. pneumoniae* MBB9 GGDEF proteins were linked to a sensory domain, presumably to modulate DGC activity in response to an environmental or metabolic signal and four of EAL domain proteins were linked to sensor domains. *Klebsiella pneumoniae* MBB9 GGDEF and EAL domain structures are shown in Table S2 in the supplementary material.

Table 4: List of domains identified in GGDEF and EAL containing proteins of the genome of *K. pneumoniae* MBB9.

	GGDEF	GGDEF-EAL	EAL
BLUF domain			2
CACHE domain	1		
CHASE domain	2	1	
CSS-motif domain			4
GAF domain	3		
GAPES4 domain		1	
HAMP domain	2		
HisKA_3	1		
MASE domain	2	2	
PAC domain	1	1	
PAS domain	1	1	
Protoglobin	1		
Membrane associated	7	5	4
Allosteric I site	7		
Probable DGC activity	11	3	
Probable PDE activity		5	8

3.4 Probable DGC enzymes in *K. pneumoniae* MBB9

Diguanylate cyclases (DGCs) are homodimeric proteins with a conserved GG(D/E)EF motif at the active site (A site). The binding of GTP to both subunits allows conversion to c-di-GMP (Figure 3). The majority (82%) of the GGDEF domain proteins of *K. pneumoniae* MBB9 had an intact conserved A site (9 GGEEF and 5 GGDEF) (Figure 4). Degenerate GGDEF A sites were present in 3 of the hybrid GGDEF-EAL proteins (CsrD, YfgF_1 and YfgF_2). In addition to the A site, many GGDEF domains possess an allosteric site (I site) characterized by the RXXD motif, located 5 amino acids upstream of the GG(D/E)EF motif, which upon binding c-di-GMP inhibits DGC activity. The I site was less well conserved, being absent from the hybrid GDDEF-EAL proteins, but present in 5 of the GGDEF proteins (Figure 4).

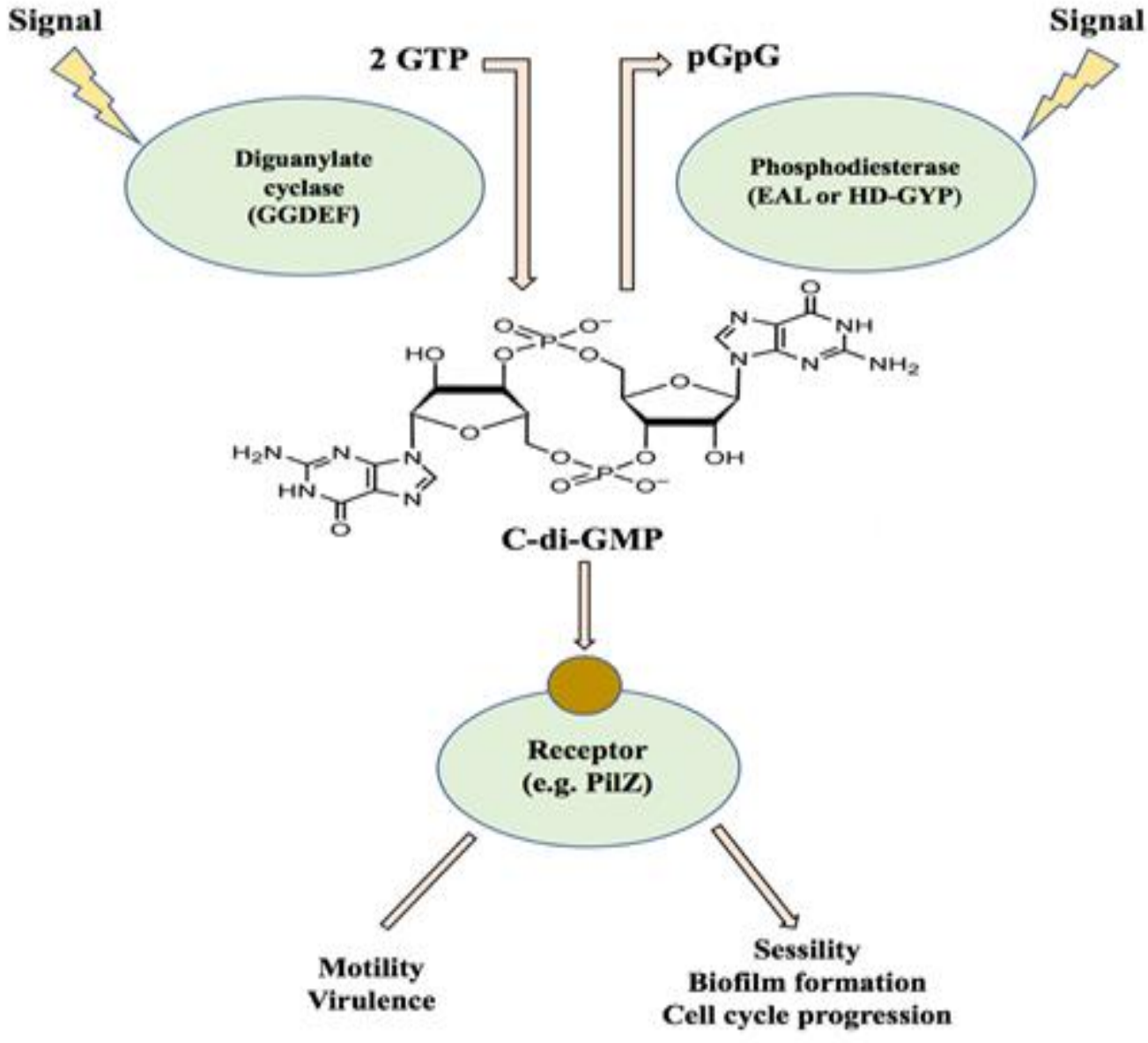

Figure 3: The c-di-GMP signalling module. Intracellular c-di-GMP is generated from two GTP molecules by diguanylate cyclases, containing GGDEF motifs, and is degraded to linear diguanylate by phosphodiesterases containing either EAL or HD-GYP domains. Cyclic di-GMP is afterward bound by a variety of effectors, including PilZ domain-containing proteins, and acts on targets affecting motility, virulence, and biofilm formation. Figure based on Schirmer and Jenal (2009).

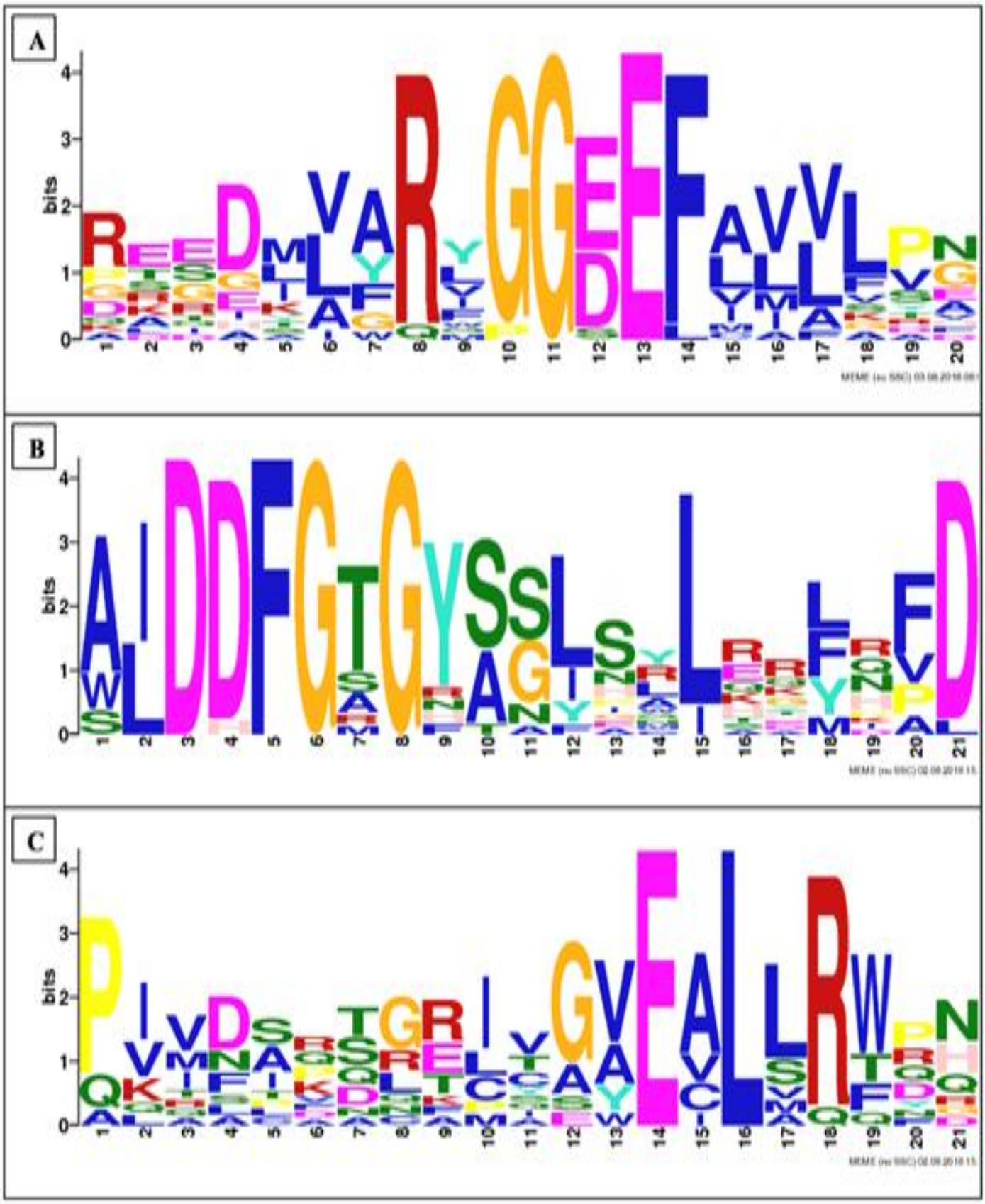

Figure 4: Logo sequences for DCG and PDE domains. Logos are shown for the active DGC domain (conserved A site; GGEEF or GGDEF) and the conserved I site motif (RxxD) (A), the PDE domain; residues conserved within the characteristic DDFGTG motifs (B) and EALxR motifs (C). Sequence logos were made using MEME analysis (http://meme-suite.org/doc/ceqlogo.html).

3.5 Probable PDE enzymes *in K. pneumoniae* MBB9

Active EAL domain proteins are characterized by 10 conserved amino acids (marked a-j in Figure 5) that contribute to c-di-GMP phosphodiesterase (PDE) activity (Tchigvintsev *et al*., 2010). Four of these 10 residues are well conserved within the characteristic DDFGTG and EALxR motifs in the primary structures of *K. pneumoniae* MBB9 EAL domains (Figure 5). The DDFGTG motif contains tandem Asp residues (locations f and g, Figure 5) that are two of six residues responsible for the coordination of the two c-di-GMP PDE active site metals (Mg^{2+} and/or Mn^{2+}) ions. One protein, BluF_2, has DHFGAG in place of DDFGTG and the inactive *E. coli* PDE YdiV, like *K. pneumoniae* MBB9 BluF_2, has a His residue at position g (Figure 5), suggesting that the *K. pneumoniae* MBB9 BluF_2 protein might lack PDE activity (Tchigvintsev *et al*., 2010).

Most variation within the DDFGTG motif was of the consensus Thr residue that is replaced by Ser, Ala or Arg in some proteins (Figure 5). The remaining four metal coordinating residues are three Glu residues (positions a, c, e and i, Figure 5) including that of the EAL motif (position a, Figure 5) and an Asn residue (position d, Figure 5). The Asn (position d, Figure 5) and one of the Glu (position e, Figure 5) residues are completely conserved in the *K. pneumoniae* MBB9 EAL domain proteins. The *K. pneumoniae* MBB9 YahA protein lacked the Glu residue of the EAL motif (position a, Figure 5) and BluF_2 had a Val residue in place of the metal coordinating Glu residue at position i (Figure 5). Three residues make direct contact with the substrate c-di-GMP, Arg at position b, Glu at position c and Asn at position d (Figure 5). The Arg at position b, which contacts one of the phosphate (c-di-GMP phosphate 2) moieties of c-di-GMP, was conserved except for YahA (EALxR motif absent) and YhjH_2 (Lys at position b, Figure 5), whereas the Asn at position d, which is involved in metal coordination as well as interacting with the opposing phosphate (c-di-GMP phosphate 1) moiety to that contacted by Arg at position b, was completely conserved (Figure 5). The alignment in the vicinity of the Glu residue at position c is more difficult to interpret, but it is likely that all the EAL domains except BluF_2 and YfgF_2 possess an appropriately located Glu residue in the 3D structure to interact with guanine base 1 of c-di-GMP (Figure 5). Downstream of the DDFGTG motif at position h (Figure 5) is a conserved Lys residue that is proposed to act with the metal ions to activate a water molecule to produce the nucleophilic hydroxyl radical that attacks the bound cyclic di-GMP (Tchigvintsev *et al*., 2010). Based upon this analysis of the EAL domains of *K. pneumoniae* MBB9 it is suggested that, excluding the regulatory protein CsrD (see below), all but BluF_2 and YahA are likely to possess c-di-GMP PDE activity. The presence Ile, Leu or Val residues at position 2 in the EAL motif is commonly found in this family of proteins, but a Cys residue in this location is unusual and occurs in two predicted *K. pneumoniae* MBB9 PDEs (YhjH_1 and YhjH_3) and it is not known what affect, if any, a Cys residue at this position might have on PDE activity.

3.6 Degenerate GGDEF-EAL

The *K. pneumoniae* MBB9 CsrD has degenerate DGC and PDE sites. *Escherichia coli* CsrD does not interact with c-di-GMP, despite its domain composition, but rather directs RNase E to degrade the small RNAs (sRNAs) csrB and csrC (Suzuki *et al*., 2006). The transcription factor CsrA binds to leader sequences in target mRNAs to regulate translation and mRNA turnover. The activity of CsrA is controlled by the intracellular concentration of the csrB/C sRNAs, which mimic CsrA binding sites and hence sequester CsrA and relieve CsrA-mediated regulation. CsrD promotes degradation of csrB/C by RNase E and thereby modulates the activity of CsrA-mediated post-transcriptional gene regulation (Suzuki *et al*., 2006). Genes coding for CsrA and the csrB/C sRNAs are present in *K. pneumoniae* MBB9 and therefore the *E. coli* Csr regulatory system is likely to operate in *K. pneumoniae* MBB9.

3.7 Sensory domains

Most of the *K. pneumoniae* MBB9 GGDEF and EAL possess recognized sensory domains (Table 4). Several *K. pneumoniae* MBB9 GGDEF proteins are associated with the structurally related CACHE (PF02743), GAF (PF01590) and PAS (PF08446) domains (Table S2 in supplementary material). All three domains are named after the proteins in which they were first identified (CACHE, calcium channels and chemotaxis receptors; GAF, cGMP PDEs, adenylate cyclase, FhlA; PAS, Per, Arnt and Sim) (Cruz *et al*., 2012). The core structure of the PAS domain consists of a five stranded anti-parallel β-sheet accompanied by several helices capable of binding a sensory cofactor (e.g. heme, flavin, 4-hydroxycinnamyl chromophore) and protein-protein interaction (Henry and Crosson, 2011). The PAS domains of *K. pneumoniae* MBB9_02530 and YdaM have PAC motifs as part of the conserved PAS domain fold. The GAF domain has a similar 3D structure to the PAS domain and is often involved in nucleotide binding to regulate the activity of partner cyclases and PDEs (Cruz *et al*., 2012). The *K. pneumoniae* MBB9 VdcA_1 protein has an N-terminal transmembrane domain (TMD) and an intracellular GAF domain as part of the TMD-HAMP-GAF-GGDEF domain organization (Table S2 in supplementary material). The HAMP domain (histidine kinases, adenylate cyclases, methyl-accepting proteins and phosphatases; PF00627) consists of an assembly of α-helices that transmit conformational changes induced by signal perception by in extracellular sensory modules (in this case the TMD) to cytoplasmic signalling domains (GGDEF) and is often found in GAF and PAS domain proteins (Matamouros *et al*., 2015).

The CACHE domain is an extracellular PAS domain that is predicted to interact with small molecules to initiate conformational changes to modulate the activity of associated intracellular activities (Cruz *et al*., 2012). The *K. pneumoniae* MBB9 DosC protein is similar (36% identical, 56% similar over 463 amino acids) to *E. coli* DgcO, which has an N-terminal heme-binding globin domain that controls the DGC activity of a C-terminal GGDEF domain in response to changes in oxygen concentration. The periplasmic ligand-binding CHASE7 domain (cyclases/histidine kinases-associated sensory extracellular; PF03924) was predicted for the GGDEF protein YedQ and a CHASE4 domain for the hybrid GGDEF-EAL protein *K. pneumoniae* MBB9_02680. An N-terminal MASE4 (membrane-associated sensor; PF17158) domain was present in the putative DGC YcdT1; it has been noted that MASE4 domains do not appear to be commonly associated with GGDEF proteins but two have been found in *K. pneumoniae* (Povolotsky and Hengge, 2016). MASE domains (MASE1; PF05231) were found in two (YfgF_1 and YfgF_2) of the hybrid GGDEF-EAL proteins. Membrane-associated domains were also predicted for the remaining four GGDEF-EAL proteins, including the CHASE4 domain (PF05228) in *K. pneumoniae* MBB9 _02680, the GAPES4 domain (PF17157) in CsrD and TMD in *K. pneumoniae* MBB9_01662. Only *K. pneumoniae* MBB9_02530 of the six hybrid GGDEF-EAL proteins was predicted to lack a membrane domain.

Four *K. pneumoniae* MBB9 EAL proteins possessed the CSS sequence motif (PF12792), which is found N-terminal to the EAL domain in many c-di-GMP PDEs, where the signal sensed remains unknown but there is evidence that the CSS domain of *Escherichia coli* PdeG acts as an inhibitor of PDE activity (Povolotsky and Hengge, 2016). Two EAL proteins had N-terminal BLUF (sensors of Blue-Light Using FAD; PF04940) domains, which resemble flavin-binding PAS domains and use a FAD cofactor to sense blue-light and redox potential (Cruz *et al*., 2012). The remaining four *K. pneumoniae* MBB9 EAL proteins lack sensory domains. Nevertheless, the widespread occurrence of sensory and TMDs associated with *K. pneumoniae* MBB9 GGDEF, GGDEF-EAL and EAL proteins suggest that most DGC and PDE activities in *K. pneumoniae* MBB9 are controlled in response to specific signals and/or location.

	a b

YhjH_2	----MVEENV---KNTSYRFVLEPAISDD-GSYHSWELLTK------DIIAPAQNTTSAS	46
YhjH_1	MNTKIFEDNILSRNDIAVRYVFQKMFSPQ-GTLVAVECLSRFDNLS---ISPED------	50
YhjH_3	MNTKITEDNILSRNDIAVRYVFQKMFSPQ-GTLVAVECLSRFDNLT---VSPEY------	50
BluF_2	----------PIVDPFACEIISWEALLRTPDGQ---SPGAY------	28
BluF_1	----------PAKRRVSSFEALIRSPTGG---SPVEM------	24
YfgF_1	----------PIQGIRGDN--YHEVLLRMEGESGELTGPNA------	29
YfgF_2	----------PIQNAEGEG--YHEILTRMRCGD-SVIMPDQ------	28
YjcC	----------PIIDIKNNRCVGAEALLRWPGFDGPVMNPAE------	31
YlaB	----------PIISLQDGKIAGAEALARWQQPDGTFLSPDI------	31
02680	----------PVVDADTLAMTGVEALLRWPRRPQGALAPDA------	31
01662	----------PIADTVTREIYGYEALVRWFHPVRGAVPPTV------	31
02530	----------LHYQAIRNIKDRRITGYEALLRWQHPQLGPIPPDV------	35
AdrB_2	----------PLQDARSGRCCGVEILLRWNNPRRGEISPEV------	31
YahA	----------	0
AdrB_1	----------PVVNAQTLRISGVEVLMRWRHPVVGEIPPDV------	31
	c d	
YhjH_2	TFSFSTLTER----------DKLALFIRQIELLSV----FDFARV--DNKPISLNIDDLL	90
YhjH_1	---FFRHATAAVRERIFLEQLALIEKHKAWFLRN----------HISATINVD---	90
YhjH_3	---FFRHATAAIRERIFLEQLALIEKHKEWFLHN----------NISATINVD---	90
BluF_2	---FAGLTGD----------DIYLADLHSKRVALSLAGKLG----L-RNKALSINLL--P	68
BluF_1	---FAAIAAE----------DRYRFDLESKAFAFSLAARLP----L-GKQQLAVNLL--P	64
YfgF_1	---FLPVAHE----------FGLSSRVDQWVIEHTLAFMDTHRRAL-PGLRLAINLS--P	73
YfgF_2	---FIPLIVQ----------FNLSQRFDMLVLETLFSSL----HQH-PGQRFSVNLL--P	68
YjcC	---FIPLAEN----------EGMIAQITDYVVDELFYEMGEFLASH-PQLYVAINLS--A	75
YlaB	---FIPLAEQ----------TGLITQLTEDIVRKIFTDLGPWLRQR-PEVHISINLS--V	75
02680	---FIAIAES----------SGLIDALGQFVLQRACSDLQP-V----DDLLLSVNIS--P	71
01662	---FIPVAEK----------IGLINTLGEWVLKTACAEAASWA----TPLKVSVNVS--P	72
02530	---FIPIAEE----------SGAIVPLGYWVLEQVCNESLEKG----LNRKVSVNIS--P	76
AdrB_2	---FIPIAEG----------DNLIIPLTRYVIAETARRLDAFPS--EPHFHIAINVA--A	74
YahA	------LAER----------TGLIIPLTRSLMAQVNAQMRPLFSKLPDGFHIGLNIS--V	42
AdrB_1	---FINLAET----------QQMIVPLTHHLLALIASDGQVLKRILPRGVKLGLNIS--P	76
	. :*:	

	e
YhjH_2	SHFILTDRY---LCDFLR---------SCKHIAL**E**INENFHEFIAGRELTALST-LAALC 137
YhjH_1	----------DHILNLLRQKDIKAKIAALTCVHF**E**VTENAEN---LLHNSLAAWQSPQDT 137
YhjH_3	----------DHILNLLRQKEIKDKIAALACVHF**E**VTENAEN---LLNNSLAAWQNPQDT 137
BluF_2	MTMVKAPNAVAFLLDEISRNDLI-----PEQIIV**E**FTEREVISRMDDFTDAVRKLKGAGI 123
BluF_1	GSLYNHPDAVGWLMDNLLAAGLR-----PEQVLI**E**VTETEVISCFDQFRKVLKALRVVGM
YfgF_1	VTL-SRSQFPQEVEALLQTYNIE-----PWQIIF**E**LTENYALSNPELVCQTLEHLRALGC 127
YfgF_2	STL-MQKDSAAQIIALFQRYRIS-----PDLITI**E**VTEEQAFSNADTSQQNLDALRAFGC 122
YjcC	SDF-HSARLISQISEKAHSYAVC-----IGQIKI**E**VTERGFI-DVAKTTPVIQAFREAGY 128
YlaB	DDL-RSPTLPTLLHDQLQHWGIA-----AEQIIL**E**ITERGFV-DPETTMPVIAHYRQAGH 128
02680	AQF-RDPAFENRVMKTVAACRFP-----PSRLQV**E**VTESYVLENPERSQAVVENLKAQGI 125
01662	IQL-MNTSLTDTIIGVLQQTGLD-----PRRLDL**E**ITESDVFNENTRSLEILSQLREQGI 126
02530	VQL-RHRSFIEKVREILMRTAYP-----VSLLEF**E**VTETAFIINKQLAFSVLHHLQKMGI 130
AdrB_2	RHF-AHGLLLHDLHNYWFSVN-P-----VQQLVV**E**LTERDVLQDGDQHM--AEHLHLKGV 125
YahA	SHI-NAPTFIDDCLHYQRGFEGK-----AVKLML**E**ITEQEPLLLNGAVVDKLNTLHSLGF 96
AdrB_1	AHL-QADSFRDDMLRFAAALPAD-----HFHVVL**E**VTERAMI-DKEKSIANFAWLHQQGF 129
	: .*..*
	fg h
YhjH_2	PVWL**DD**FGRGRTSFPLLERFRFDCV**K**VDKDYFWDKENDPAFPGLLQSI----HTLTSHVI 193
YhjH_1	SLWL**DD**FGSGYAGINAIRGYHFDYV**K**IDKDFFWHLMRKESGRQLMDALVTFLSRNHHN VI 197
YhjH_3	SLWL**DD**FGSGYAGINAIRGYHFDYV**K**IDKDFFWHLMRKESGRQLMDALVTFLSRNHHN VI 197
BluF_2	NLAI**D**HFGAGFAGLSLLAQYQPDRI**K**IDHELIRNIHQDGPRQSIVQAIIKCCTSLEIAVS 183
BluF_1	KLAI**DD**FGAGYSGLSLLTRFQPDKI**K**VDAELVRDIHISGTKQAIVASVVRCCEDLGITVV
YfgF_1	RVAI**DD**FGTGYASYARLKTMNVDIL**K**IDGSFIRNLLASSLDYQVVDSICRLARMKNMQV V 187
YfgF_2	AIAI**DD**FGTGYANYERLKHLQADII**K**IDGCFVRDILTDPLDAIMVKSIVEMARAKQMSVV
YjcC	EIAI**DD**FGTGYSNLHNLHALNVDIL**K**IDKTFVDTLTTNNTSHLIAEHIIEMARGLRLKTI

	188
YlaB	RISI**DD**FGTGYSSLSYLQKLDVDTL**K**IDKSFVDTLEYR----PLTPHIIEMAKALNLATV
	184
02680	AVAL**DD**FGTGYSSIGYLRRFRFDSL**K**IDKSLAGRVDSDEQAAEMVRGTVRIARALGMTV
	V 185
01662	QISI**DD**FGTGYSSLSRLSYFPFDKI**K**IDRSFVINIPEQKDDLDIVRLIISMGKSLHMRIV
	186
02530	SIAL**DD**FGTGYSSLSMLRDFHFDVI**K**LDRSFMLDVESNPQVRSFVRAIISLGNSINTPLI
	190
AdrB_ 2	QLAI**DD**FGTGNSSLSWLEKLRPDVL**K**IDRSFTSSVGIDSVNATVTDIIIALADRLNIVTV
	185
YahA	SIAL**DD**FGTGYSGLSCLHELIFDYI**K**IDQSFVGRVTGEAPASKLLDCVIEMARTLSLRII
	156
AdrB_ 1	EIAI**DD**FGTGHSALIYLERYNFDYL**K**IDRGFVQAIGTETVTSPVLDAVLTLSRRLKLMTV
	: :*.** * : : * :*:* .
	i **j**
YhjH_ 2	V**E**GIETEKQKQLISAAGDIIG**Q**GRYWKDEYIFL----CC---------- 228
YhjH_ 1	I**E**GVESEAHKEWLQGMEWFAI**Q**GHYWREV-SIE-QLVADDIAM---------- 238
YhjH_ 3	I**E**GVESEDHKKWLQGMEWFAI**Q**GHYWQEV-SIE-QLVADDITR---------- 238
BluF_2	AVGVERAEEWMWLESAGISQF**Q**GNLFASARLGGLPAVAWPEKK----------226
BluF_1	A**E**GVETIEEWCWLQSVGIRLF**Q**GFLFSRPCLNGIAEICWPVARQATDL----------
	227
YfgF_1	A**E**YVESPEIRQAVIALGIDYL**Q**GYDIGVPVPLA-QLAEGMTA---------- 228
YfgF_2	A**E**YVESEPQKARLLELGVNYL**Q**GYLVGKPQPLG-E---------- 216
YjcC	A**E**GVETPEQVSWLYKRGVQFC**Q**GWLFAKAMPAR-EFMQWLANAPTPISRPQPPRHAEI
YlaB	A**E**GVETESQRDWLRQHGVQYA**Q**GWLYSKALPKE-QFILWAENNLHVH----------
	230
02680	A**E**GVEDPQQLTLLRRAGCDRL**Q**GYYFSKPMPIA-DLLQRRQSQG---------- 228
01662	A**E**GVETEEQLTSLQALGCDLV**Q**GYLIGKPSPLR---------- 219
02530	A**E**GVETAGQLQILEEEGCDEM**Q**GFLFGEPVDIK-HLPPSS---------- 229
AdrB_ 2	A**E**GVETLEQESYLRGHGVDVL**Q**GFYYARPMPIE-AFPAWLADREGQKSEGGE------
	236
YahA	A**E**GVETEAQRDYLNRQNIHLL**Q**GYYFWKPMPYV-ALVMLLLSKPKARIVEE-------
	206
AdrB_ 1	A**E**GVETQEQAEWLRAQGVNFL**Q**GYWISRPLSLE-ALVAAHDE-PANYFTTR-------
	238
	:* : **

Figure 5: A CLUSTAL O(1.2.4) multiple sequence alignment of *K. pneumoniae* MBB9 EAL domains. Structure-based sequence alignment of the EAL domains from *K. pneumoniae* MBB9 proteins. Ten conserved EAL domain residues are colored and marked a-j. Asterisk (*) indicates positions which have a

single, fully conserved residue, colon (:) indicates conservation between groups of strongly similar properties - scoring > 0.5 in the Gonnet PAM 250 matrix and period (.) indicates conservation between groups of weakly similar properties-scoring =< 0.5 in the Gonnet PAM 250 matrix.

4. Discussion

The comparative genomic analysis allows phenotypic differences between strains and species to be associated with changes in the chromosomes (Carver *et al*., 2005). *Klebsiella pneumoniae* MBB9 harboured multiple copies of GGDEF and EAL domain proteins, either separately or together, forming hybrid proteins that have both GGDEF and EAL domains (Cruz *et al*., 2012). A previous study of three *K. pneumoniae* genomes, one environmental strain and two clinical isolates, showed that most of GGDEF and EAL domain-containing genes were shared among the three strains but that some were unique to a particular strain, suggesting that the existence of various proteins is indicative of a complex c-di-GMP network in *K. pneumoniae* (Cruz *et al*., 2012). The presence of such genes in *K. pneumoniae* MBB9 is not surprising as it is known that proteins with EAL or GGDEF usually exist in both gram-negative and gram-positive bacteria, but they are more copious in gram-negative species (Castiglione *et al*., 2011). The remarkable multiplicity of GGDEF and EAL domains and their association with various proteins suggest that many different signals can be integrated into the cellular c-di-GMP pool and that different processes can be targeted and regulated in parallel (Tchigvintsev *et al*., 2010). The existence of such domains might suggest that these domains have a role in *K. pneumoniae* MBB9 biofilm formation since they can regulate the c-di-GMP level which in turn controls a wide range of functions including the formation of bacterial biofilm (Sisti *et al*., 2013). Besides, six genes that coding for GGDEF and EAL proteins were not present in the genome sequence of *K. pneumoniae* MBB9 compared to *K. pneumoniae* 342, suggesting that these genes might be exclusive in *K. pneumoniae* 342. Similarly, Cruz *et al*. (2012) have found that *K. pneumoniae* 342 had three genes coding for GGDEF and EAL proteins compared with two *K. pneumoniae* clinical isolates. This was interpreted as suggesting that these genes could be important for interactions with plants and the ability to grow like a plant endophyte. However, it is difficult to identify the source of pathogens, such as *K. pneumoniae* MBB9 and the pathways by which they enter the water resources (Pandey *et al*., 2014).

Several studies have established that proteins containing GGDEF amino acid sequence motifs often have DGC activity, while proteins including EAL amino acid sequence motifs often possess PDE activity (Rakshe *et al*., 2011). Analysis of the GGDEF domains of *K. pneumoniae* MBB9 showed that the majority of such domains had a conserved A site, suggesting that they are catalytically active. However, in hybrid GGDEF-EAL proteins, such as CsrD, YfgF_1 and YfgF_2, degenerate GGDEF A sites were found. This might suggest that they are inactive and do not directly synthesize or degrade c-di-GMP but might have used different functions, either as c-di-GMP binding effector proteins or participate in other macromolecular interactions with no involvement of c-di-GMP at all (Cruz *et al*., 2012). In different bacteria, various GGDEF degenerate proteins have been shown to lack DGC activity but in many cases have adopted different functions, some of which involve binding of c-di-GMP (Cruz *et al*., 2012). Most of the *K. pneumoniae* MBB9 GGDEF domains were found to possess the regulatory I site, but this was absent from the hybrid GDDEF-EAL proteins. The I sites have been shown to be less common in catalytically active DGC hybrid proteins, suggesting that these proteins might have lower activities compared to single-domain DGCs proteins (Cruz *et al*., 2012). In addition to GGDEF domains, the analysis of the EAL domains of *K. pneumoniae* MBB9 suggests that all but BluF_2 and YahA are likely to possess c-di-GMP PDE activity and might be catalytically active. When the EAL domains of YahA and BluF_2 were aligned with the enzymatically active EAL domains, YahA was found to lack EALxR motifs including Glu residue of the EAL motif and BluF_2 was found to have a Val residue in place of Glu residue and had a His residue in the DDFGAG motif (DHFGTG). A similarly located His residue in *E. coli* YdiV inactivates PDE activity

(Tchigvintsev *et al*., 2010). In bacteria, such as *Gluconacetobacter xylinus*, the inactive PDEs DgcA1 and DgcA3 contained at least one substitution in the most conserved DDFGTG motif that presents in the active EAL domains (Schmidt *et al*., 2005). Thus, the absence of EALxR motifs and the presence of a His residue in the most conserved DDFGTG motif might contribute to the inactivity of the EAL domains in such proteins.

One of the most interesting features of the enzymes for modulating intracellular c-di-GMP levels is their modular structure characterized by the presence of additional input sensory domains (Cruz *et al*., 2012). In *K. pneumoniae* MBB9, the majority of the GGDEF and EAL-containing proteins contained sensor domains. Some domains were found exclusively in GGDEF proteins (CACHE, GAF, HAMP, HisKA_3 and Protoglobin) or EAL proteins (BLUF and CSS), while others were shared or found in hybrid proteins (CHASE, GAPES4, MASE, PAC, PAS and membrane-associated). Besides, some sensor domains, such as REC (receiving domain with phosphoacceptor site) which is involved in DGC protein activation in organisms, such as *Caulobacter crescentus* and *Pseudomonas* was not found in *K. pneumoniae* MBB9 (Cruz *et al*., 2012). As in other bacteria, the different sensor domains might suggest a various range of environmental stimuli associated with the regulatory responses in *K. pneumoniae* MBB9.

Acknowledgements

Special thanks to the entire group in the Department of Molecular Biology and Biotechnology at the University of Sheffield and in particular Prof. Milton Wainwright and Prof. Jeff Green for their assistance.

Funding

This research did not receive any specific grant from funding agencies in the public, commercial, or not-for-profit sectors.

Conflicts of Interest

The author declares no conflict of interest.

References:

1. ALCÁNTAR-CURIEL, M. D. BLACKBURN, D. SALDAÑA, Z. GAYOSSO-VÁZQUEZ, C. IOVINE, N., DE LA CRUZ, M. A., and GIRÓN, J. A. (2013). Multi-functional analysis of *Klebsiella pneumoniae* fimbrial types in adherence and biofilm formation. *Virulence*, 4**,** 129-138.
2. ALOTAIBI, G. F. (2020). Occurrence of Potentially Pathogenic Bacteria in Epilithic Biofilm Forming Bacteria isolated from Porter Brook River-stones, Sheffield, UK. *Saudi Journal of Biological Sciences*, *27*(12), 3405.
3. APHA, A. J. I. WASHINGTON. (1998). Standard methods for the examination of water and wastewater, American Public Health Association.
4. BERGEY, D. H., and HOLT, J. G. (1994). *Bergey's manual of determinative bacteriology*, 9th edition, Williams and Wilkins. Baltimore, USA.
5. CARVER, T. J., RUTHERFORD, K. M., BERRIMAN, M., RAJANDREAM, M.A., BARRELL, B. G., and PARKHILL, J. (2005). ACT: the Artemis Comparison Tool. *Bioinformatics (Oxford, England)*, 21**,** 3422-3423.
6. CASTIGLIONE, N., STELITANO, V., RINALDO, S., GIARDINA, G., CARUSO, M., and CUTRUZZOLÀ, F. (2011). Metabolism of cyclic-di-GMP in bacterial biofilms: from a general overview to biotechnological applications.
7. CHRISTENSEN, G. D., BALDASSARRI, L., and SIMPSON, W. A. (1995). Methods for studying microbial colonization of plastics. *Methods in enzymology*, 253, 477-500.

8. CHRISTENSEN, G. D., SIMPSON, W. A., YOUNGER, J. J., BADDOUR, L. M., BARRETT, F. F., MELTON, D. M., and BEACHEY, E. H. (1985). Adherence of coagulase-negative *staphylococci* to plastic tissue culture plates: a quantitative model for the adherence of *staphylococci* to medical devices. *Journal of clinical microbiology,* 22**,** 996-1006.
9. COTTER, P. A., and STIBITZ, S. (2007). Cyclic-di-GMP mediated regulation of virulence and biofilm formation. *Current Opinion in Microbiology,* 10**,** 17-23.
10. CRUZ, D. P., HUERTAS, M. G., LOZANO, M., ZÁRATE, L., and ZAMBRANO, M. M. (2012). Comparative analysis of diguanylate cyclase and phosphodiesterase genes in *Klebsiella pneumoniae*. *BMC Microbiology,* 12, 139.
11. GAO, X., MATTHEWS, P. M., HAMMAD, L. A., DANN III, C. E., MUKHERJEE, S., and KEARNS, D. B. (2013). Functional characterization of core components of the *Bacillus subtilis* cyclic-di-GMP signaling pathway. *Journal of Bacteriology,* 195, 4782-4792.
12. GOMES, L. C. F. (2012). Optimization of cultivation conditions for *E. coli* biofilm formation in microtiter plates.
13. HENRY, J. T., and CROSSON, S. (2011). Ligand-binding PAS domains in a genomic, cellular, and structural context. *Annual Review of Microbiology*,65**,** 261-286.
14. JOHNSON, J. G., and CLEGG, S. (2010). Role of MrkJ, a phosphodiesterase, in type 3 fimbrial expression and biofilm formation in *Klebsiella pneumoniae*. *Journal of Bacteriology*, 192**,** 3944-3950.
15. JONATHAN, J. W., JI, Y., ABIGAIL, C., JACINTA, L. G., KIRSTY, R. S., HANWEI, C., ROSALIA, C., CATHERINE, E. J., CYNTHIA, B. W., MARK, A. S., MARY, L. C. C., ZHAO-XUN, L., ODILIA, L. W., ADAM, W. J., TREVOR, L., and RICHARD, A. S. (2011). MrkH, a novel c-di-GMP dependent transcriptional activator, controls *Klebsiella pneumoniae* biofilm formation by regulating type 3 fimbriae expression. *PLoS Pathogens,* 7**,** e1002204.
16. MARVIN, W., BANGERA, M. G., ROGER, E. B., MATTHEW, R. P., GAIL, M. T., STEPHEN, L., and GREENBERG, E. P. (2001). Gene expression in *Pseudomonas aeruginosa* biofilms. *Nature,* 413**,** 860.
17. MATAMOUROS, S., HAGER, K., and MILLER, S. (2015). HAMP domain rotation and tilting movements associated with signal transduction in the PhoQ Sensor Kinase. *Bimonthly peer-reviewed open access scientific journal,* 6, e00616-15.
18. MURPHY, C., MORTENSEN, M., KROGFELT, K., and CLEGG, S. (2013). Role of *Klebsiella pneumoniae* type 1 and type 3 fimbriae in colonizing silicone tubes implanted into the bladders of mice as a model of catheter-associated urinary tract infections. *Infection and Immunity,* 81**,** 3009-3017.
19. O'TOOLE, G. A., and KOLTER, R. (1998). Initiation of biofilm formation in *Pseudomonas fluorescens* WCS365 proceeds via multiple, convergent signalling pathways: a genetic analysis. *Molecular microbiology*, 28, 449-461.
20. PANDEY, P., KASS, P., SOUPIR, M., BISWAS, S., and SINGH, V. (2014). Contamination of water resources by pathogenic bacteria. *AMB Express,* 4**,** 1-16.
21. POVOLOTSKY, T., and HENGGE, R. (2016). Genome-based comparison of cyclic-di-GMP signaling in pathogenic and commensal *Escherichia coli* strains. *Journal of Bacteriology,* 198**,** 111-126.
22. RAKSHE, S., SPORMANN, A. M., and LEFF, M. (2011). Indirect modulation of the intracellular c-di-GMP level in *Shewanella oneidensis* MR-1 by MxdA. *Applied and Environmental Microbiology,* 77**,** 2196-2198.

23. SALONI, S., KUSUM, H., and SANJAY, C. (2012). Susceptibility of different phases of biofilm of *Klebsiella pneumoniae* to three different antibiotics. *The Journal of Antibiotics,* 66**,** 61.
24. SCHMID, N., SUPPIGER, A., STEINER, E., PESSI, G., KAEVER, V., FAZLI, M., TOLKER-NIELSEN, T., JENAL, U., and EBERL, L. (2017). High intracellular c-di-GMP levels antagonize quorum sensing and virulence gene expression in *Burkholderia cenocepacia* H111. *Microbiology (Reading, England),* 163**,** 754-764.
25. SCHMIDT, A. J., RYJENKOV, D. A., and GOMELSKY, M. (2005). The ubiquitous protein domain EAL is a cyclic diguanylate-specific phosphodiesterase: enzymatically active and inactive EAL domains. *Journal of Bacteriology,* 187**,** 4774-4781.
26. SCHROLL, C., KROGFELT, K. A., STRUVE, C., and BARKEN, K. B. (2010). Role of type 1 and type 3 fimbriae in *Klebsiella pneumoniae* biofilm formation. *BMC Microbiology,* 10.
27. SCHURTZ SEBGHATI, T. A., CLEGG, S., KORHONEN, T. K., and HORNICK, D. B. (1998). Characterization of the type 3 fimbrial adhesins of *Klebsiella* strains. *Infection and Immunity,* 66**,** 2887-2894.
28. SISTI, F., HOZBOR, D., FERNÁNDEZ, J., HA, D.G., and TOOLE, G. A. (2013). Cyclic-di-GMP signalling regulates motility and biofilm formation in *Bordetella bronchiseptica*. *Microbiology (United Kingdom),* 159**,** 869-879.
29. STELITANO, V., GIARDINA, G., PAIARDINI, A., CASTIGLIONE, N., CUTRUZZOLA, F., and RINALDO, S. (2013). Cyclic-di-GMP hydrolysis by *Pseudomonas aeruginosa* HD-GYP phosphodiesterase: analysis of the reaction mechanism and novel roles for pGpG: e74920. *PLoS ONE,* 8, e74920.
30. SUZUKI, K., BABITZKE, P., KUSHNER, S., and ROMEO, T. (2006). Identification of a novel regulatory protein (CsrD) that targets the global regulatory RNAs CsrB and CsrC for degradation by RNase E. *Genes and Development,* 20**,** 2605-2617.
31. TCHIGVINTSEV, A., XU, X., SINGER, A., CHANG, C., BROWN, G., PROUDFOOT, M., CUI, H., FLICK, R., ANDERSON, W. F., JOACHIMIAK, A., GALPERIN, M. Y., SAVCHENKO, A., and YAKUNIN, A. F. (2010). Structural insight into the mechanism of c-di-GMP hydrolysis by EAL domain phosphodiesterases. *Journal of Molecular Biology,* 402**,** 524-538.
32. VALENTINI, M., and FILLOUX, A. (2016). Biofilms and cyclic-di-GMP (c-di-GMP) signaling: lessons from *Pseudomonas aeruginosa* and other bacteria. *The Journal of Biological Chemistry,* 291**,** 12547-12555.
33. VUOTTO, C., LONGO, F., BALICE, M., DONELLI, G., and VARALDO, P. (2014). Antibiotic resistance related to biofilm formation in *Klebsiella pneumoniae*. Basel: *Pathogens*, 3, 743-758.

How to cite this article: Alotaibi, G. F., & Green, J. (2023). Identification and Characterisation of a cyclic di-GMP-specific Diguanylate Cyclase and Phosphodiesterase Genes in Klebsiella Pneumoniae MBB9 . Journal of Current Medical Research and Opinion, 6(08), 1649-1670. https://doi.org/10.52845/CMRO/2023/6-8-4

Supplementary material

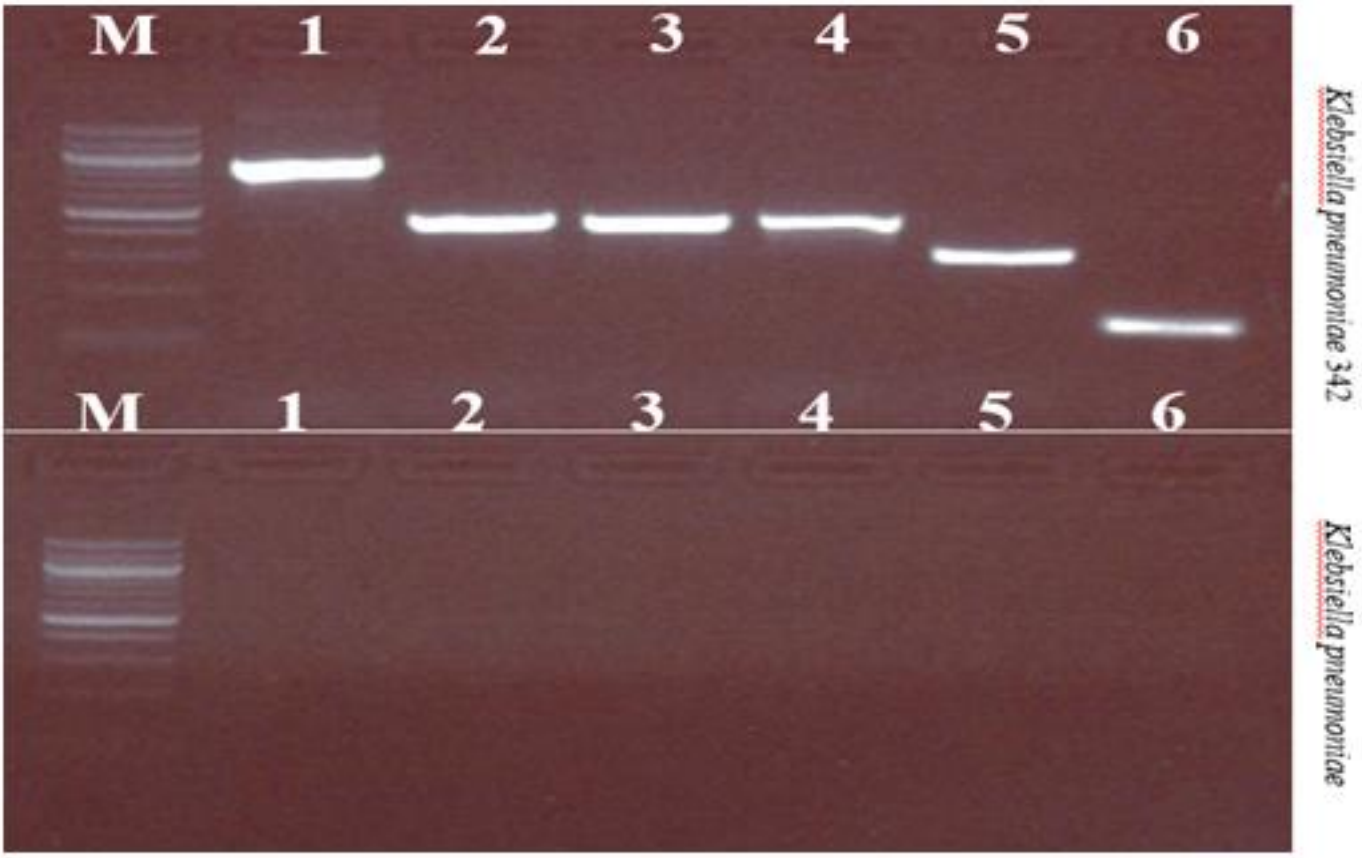

Figure S1: Amplification of genes coding for GGDEF and EAL proteins in *K. pneumoniae* 342. The PCR products were separated on 1% agarose gel and visualized using SYBR Safe DNA Gel Stain. Lane M, DNA marker, from top to bottom: 1,517, 1200, 1000, 900, 800, 700, 600, 517, 400, 300, 200 and 100 base pairs; lanes 1-6, PCR amplifications; 1: *KPK_3563*, 2: *KPK_3558*, 3: *KPK_3392*, 4: *KPK_3355*, 5: *KPK_3356* and 6: *KPK_0810*. The PCR products matched their expected sizes.